

Layer-dependent photoemission study of magnetically ordered Sm monolayers on Fe(100)

E. Vescovo

Institut für Festkörperforschung des Forschungszentrums Jülich, D-5170 Jülich, Germany

R. Rochow

Heinrich-Heine Universität Düsseldorf, D-4000 Düsseldorf, Germany

T. Kachel

Berliner Elektronenspeicherring-Gesellschaft für Synchrotronstrahlung m.b.H. (Bessy), Lentzeallee 100, D-1000 Berlin 33, Germany

C. Carbone

Institut für Festkörperforschung des Forschungszentrums Jülich, D-5170 Jülich, Germany

(Received 15 January 1992)

Sm overlayers on Fe(100) have been studied by use of spin-resolved photoemission with synchrotron radiation, low-energy electron diffraction, and Auger spectroscopy. Sm grows on Fe(100) in the layer-by-layer mode. Sm is trivalent ($4f^5$ electronic configuration) for coverages up to 1 monolayer. At higher coverage, Sm is mixed valent, with a divalent ($4f^6$ electronic configuration) surface monolayer on top of the trivalent underlying layers. The surface valence transition of the topmost atomic layer allows one to determine the spin polarization of the individual Sm atomic layers. Spin-resolved photoemission measurements show that the Sm atomic layers near the interface are magnetically ordered, with a ferromagnetic component in the interface plane. The in-plane spin moment of the $4f$ electrons is antiparallel to the Fe $3d$ majority-spin direction. The in-plane ferromagnetic ordering is found to decrease rapidly within the overlayer and to vanish three atomic layers away from the interface.

I. INTRODUCTION

Recent developments in the synthesis of layer and multilayer structures offer new models for the study of rare-earth- $3d$ -transition-metal (RE-TM) systems. The unusual properties of RE-TM layered systems are of great interest for application in information technology as magnetic storage media. From a fundamental standpoint, the electronic origin of the RE-TM magnetic properties is quite complicated, depending on the coupling between the itinerant TM $3d$ and the localized RE $4f$ polarized states. For example, it is well known that amorphous rare-earth-transition-metal films present a perpendicular magnetic anisotropy but the fundamental physical origin of this property has remained until now controversial.¹ The experimental information on the electronic and microscopic structure of RE-TM layered systems on an atomic scale is still very limited. Shan *et al.* have recently studied the magnetic anisotropies and interface coupling in RE-TM multilayers as a function of layer thickness. They conclude that single-ion anisotropy is the major contributor to the observed perpendicular anisotropy of Dy/Co multilayers and similar systems.² Fu, Mansuripur, and Meystre, on the basis of model calculation attribute the origin of the anisotropy to the RE-TM pairs.³ Landolt and co-workers have studied with spin-polarized Auger spectroscopy the interface coupling between Fe and Gd.⁴ They found that the Gd moment couples antiparallel to that of the Fe substrate. This work was confirmed and extended to other RE elements in following studies by spin-resolved photoemission and Auger

spectroscopy.^{5,6}

In this paper we present a study of the electronic and magnetic structure of Sm ultrathin layers on an Fe(100) single crystal. The main aim of this work is to provide a microscopic characterization of the electronic and magnetic structure at a RE-TM interface. Photoemission, being highly surface sensitive, is well suited to study interface phenomena on an atomic scale. Sm is characterized in the metallic form by a surface valence transition, which allows one to separate the surface signal from the bulk one. We will show that Sm on Fe(100) is a convenient model case since the surface valence transition allows us to resolve the contribution from sequential atomic layers.

This paper is organized as follows. In Sec. II we present a short account of the experiment procedure. In Sec. III we discuss the growth mode and the Sm electronic structure. In Sec. IV we discuss the spin-resolved photoemission spectra and the magnetic order of the overlayer. Finally the conclusions of this work are summarized in Sec. V.

II. EXPERIMENT

Here we report on the main features of the spin-resolved photoemission apparatus and on the experimental procedures. The spin-resolved photoemission system consists of two interconnected chambers. The first chamber is an ultrahigh-vacuum chamber (base pressure 2×10^{-10} mbar) equipped with a photoelectron energy analyzer and conventional facilities for the preparation of

single-crystal surfaces. The second chamber contains a Mott polarimeter. Clean Fe(100) surfaces were obtained by evaporating a thick [more than 10 monolayer (ML)] Fe layer on an Fe-3 at. % Si single crystal, whose surface was previously prepared by repeated cycles of heating (about 700 K) and Ar⁺ sputtering (1 kV, 4 μ A). Pure Fe (99.999% purity) has been evaporated from an electron-beam-heated Fe rod contained in a water-cooled crucible. After a careful degassing procedure, Fe evaporations could be performed at a pressure below 8×10^{-10} mbar. No contaminants were detected by Auger and photoemission spectroscopy on the freshly prepared Fe surface. The Fe crystal surface showed a very good low-energy electron diffraction (LEED) pattern with sharp diffraction spots on a low background. Sm layers were deposited *in situ* by evaporation from a resistively heated W basket. During Sm evaporation the pressure rose to 8×10^{-10} mbar. The Sm deposition rate, typically 1 $\text{\AA}/\text{min}$, was calibrated with a quartz oscillator microbalance. Throughout this paper, one monolayer is defined as the mass equivalent of one atomic layer calculated from the Sm bulk density, assuming an interlayer spacing of 3 \AA . All the evaporations and measurements were performed on the substrate at room temperature. The sample was shaped as a picture frame, with a magnetizing coil wrapped around one of its legs. The Fe sample was measured in remanence with the magnetization along the in-plane $\langle 100 \rangle$ easy axis direction.

The photoemission experiment was performed with monochromatized *s*-polarized radiation from the BESSY-TGM5 undulator beam line.⁷ The photoemission spectra were measured for normal electron emission with a 90° spherical analyzer. The total energy resolution was about 0.3–0.4 eV. The spin analysis was performed by Mott scattering at 100 kV on a thin Au target. The geometry of the system allows the measurement of the projection of the spin polarization vector along the in-plane Fe $\langle 100 \rangle$ axis: $P(E) = [I^\uparrow(E) - I^\downarrow(E)] / [I^\uparrow(E) + I^\downarrow(E)]$ where $I^{\uparrow(\downarrow)}$ are the spin-resolved energy distribution curves (SREDC's) for majority (minority) -spin electrons. The measurement of the spin integrated energy distribution curve $I_0(E) = I^\uparrow(E) + I^\downarrow(E)$ along with the spin polarization $P(E)$ then allows one to obtain the SREDC's: $I^{\uparrow(\downarrow)} = I_0(E)[1 \pm P(E)]/2$.

III. OVERLAYER GROWTH AND ELECTRONIC STRUCTURE

A. Growth mode

In order to determine the growth mode of Sm overlayers on the Fe(100) substrate, we monitored the peak-to-peak height ratio between the adsorbate Sm $N_{4,5}VV$ (103 eV) and the substrate Fe $M_{2,3}VV$ (47 eV) Auger lines as a function of Sm coverage. The Auger ratio versus coverage turns out to be in good agreement with the layer-by-layer growth mode, at least for the first 4 ML of Sm. Moreover we measured the Fe 3*p* photoelectron spectra. The binding energy and line shape of the Fe 3*p* core levels remain unaffected upon Sm deposition. The absence of chemically shifted components in the core-level spectra gives a further indication that no Sm-Fe in-

termixing or Fe surface segregation take place. Other evidence in support of the layer-by-layer growth mode is given by the valence-band photoemission spectra, which will be discussed in detail in the following paragraph.

The overlayer growth has been further investigated by low-energy electron diffraction. The clean Fe(100) surface shows a sharp (1 \times 1) LEED pattern. No extra structure induced by Sm deposition could be detected in the diffraction pattern. Instead, the diffuse background was found to increase already with Sm coverage below 0.5 ML. With 61-eV primary electron energy the diffraction pattern disappears with Sm coverages near 1 ML. We therefore conclude that Sm overlayers on Fe(100) do not exhibit long-range atomic order.

B. Development of the electronic structure versus coverage

The study of the electronic structure of Sm overlayers on Fe(100) is interesting *per se*, as proved by the several recent studies on Sm/metal single crystals.⁸ The Sm atom is divalent with a $4f^6(5d6s)^2$ configuration. In the metallic state Sm becomes trivalent [$4f^5(5d6s)^3$ valence configuration] being energetically favorable to promote an electron from the localized 4*f* level into the conduction band. However, the divalent and the trivalent configurations have very similar energy in the metal. Johansson⁹ suggested that the reduced atomic coordination at the surface of the solid could maintain the Sm surface atoms in the divalent configuration. This forecast has been experimentally confirmed by means of various spectroscopic techniques.¹⁰ Similarly, recent theoretical and experimental works have shown that the Sm valence configuration in ultrathin overlayer and dilute adsorption systems depends critically on the chemical environments. The ground state is determined by a competition between the electronic hybridization and the 4*f* promotion energy.

In order to study the electronic structure of the Sm/Fe system, we have measured valence-band photoemission spectra as a function of coverage. We took advantage of the tunability of the photon energy through the Sm 4*d* core level threshold, where the $4d \rightarrow 4f$ giant resonance occurs.¹¹ The resonance can be used as an amplifier of the Sm 4*f* signal to greatly enhance the sensitivity of the measurements down to very low coverage (about 0.1 ML Sm). Also, by tuning the photon energy across the resonance, the Fe and Sm emissions can be disentangled from each other. As an example, we show in Fig. 1 the spectra of 1.8 ML Sm on Fe measured across the resonance region. The spectrum measured with 125-eV photon energy (antiresonance) is dominated by the Fe 3*d* emission near the Fermi level (see also Fig. 2). The Sm spectral features, between 4 and 10 eV, are very weak because the Sm 4*f* cross sections are extremely low at this photon energy. The antiresonance spectra show little change with Sm coverage indicating that the Fe interface electronic structure is not strongly affected by Sm deposition.

The divalent and trivalent 4*f* emissions resonate at different photon energy, reflecting the different $4d \rightarrow 4f$ multiplet excitation energies for the two configurations.

The Sm²⁺ emission has its maximum intensity at 135-eV photon energy, as shown in Fig. 1 by the resonating

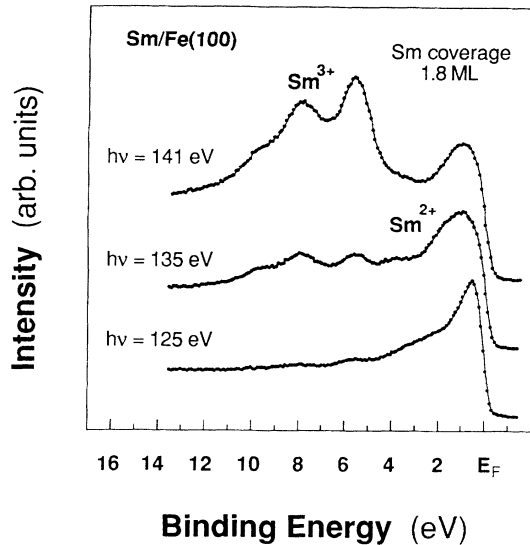


FIG. 1. Photon energy dependence of the Sm 4f spectral features through the $4d \rightarrow 4f$ threshold.

multiplet split features ($4f^5$ final state) in the 0–5-eV binding energy region.

The Sm^{3+} 4f emission is on resonance at 141 eV. The characteristic Sm^{3+} 4f multiplets ($4f^4$ final state) are found in the 5–12-eV binding energy range. At 141-eV photon energy the Sm^{2+} emission contributes still to most of the spectral features near the Fermi level, because the divalent resonance has a broad line shape.¹²

In Fig. 2 we show a set of representative spectra measured at 141-eV photon energy (Sm^{3+} and Sm^{2+} resonance) for increasing Sm coverage.

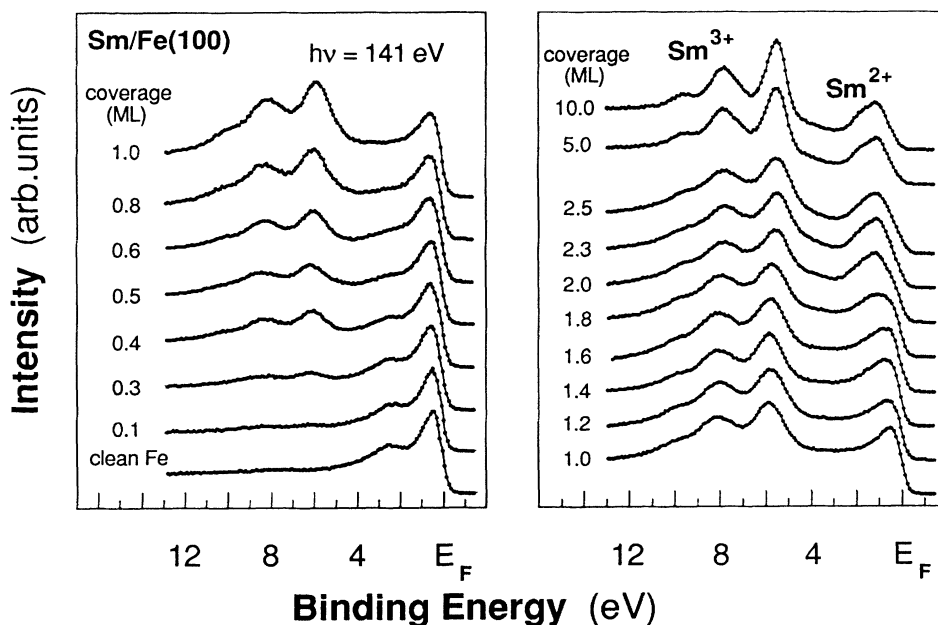


FIG. 2. Stack of photoemission spectra of Sm/Fe(100) as a function of Sm coverage. The photon energy ($h\nu=141$ eV) is at the maximum of the $4d \rightarrow 4f$ resonance for the Sm trivalent configuration.

An analogous set of spectra measured at the divalent resonant energy is shown in Fig. 3. Figures 2 and 3 contain two main pieces of information on the Sm valence configuration which will be discussed in detail in the following: Sm^{3+} emission is seen in the submonolayer spectra; the Sm^{2+} emission appears in the spectra at coverages above 1 ML (see also the development of the divalent¹³ multiplet feature at 4-eV binding energy in Fig. 3).

In order to discuss the evolution of the Sm valence configuration as a function of the coverage, we plot in Fig. 4 the ratio of the areas under the divalent (2+) and the trivalent (3+) peaks [$I(\text{Sm}^{2+})/I(\text{Sm}^{3+})$]. These values are obtained from the on-resonance spectra at 141-eV photon energy. To extract the 4f contribution the antiresonance spectra were subtracted from the corresponding on-resonance spectra. All the spectral intensities were normalized to the incident photon flux.

At submonolayer coverage the Sm^{3+} component is by far more intense than the Sm^{2+} one. Little or no Sm^{2+} emission appears in the difference spectra in this coverage range. The (weakly resonating) Sm 5d emission, overlapping the Sm^{2+} binding energy region, possibly accounts for the small fraction attributed to Sm^{2+} below 1 ML in Fig. 4. A steep increase of the divalent intensity takes place between 1 and 2 ML coverage. The $I(\text{Sm}^{2+})/I(\text{Sm}^{3+})$ ratio reaches its maximum just near the completion of the second atomic layer. Above 2 ML coverage the $I(\text{Sm}^{2+})/I(\text{Sm}^{3+})$ ratio decreases towards a saturation value which is approximately reached at 5 ML thickness.

The curve of Fig. 4 can be readily understood assuming that the first deposited monolayer forms a trivalent inter-

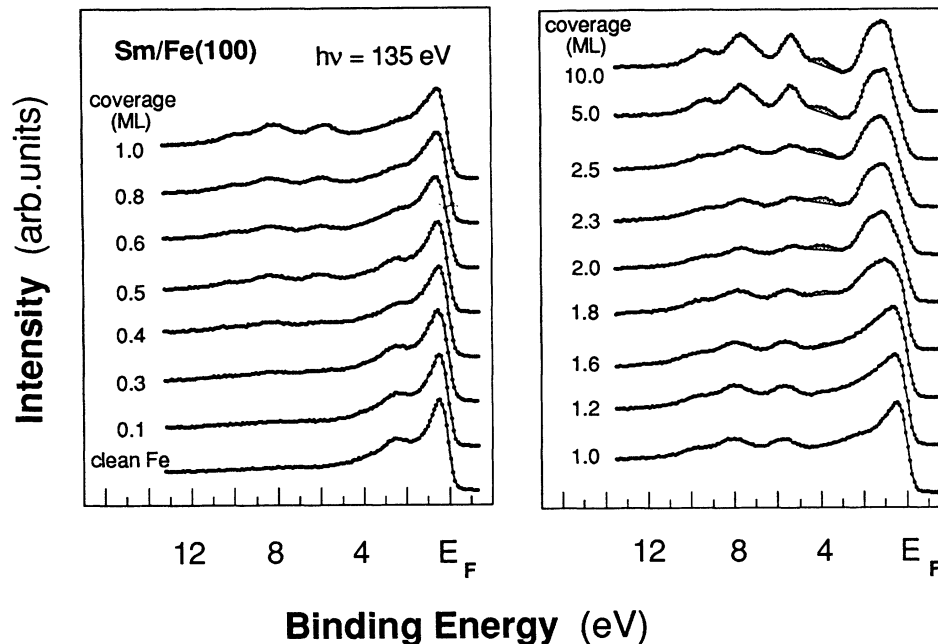


FIG. 3. Stack of photoemission spectra of Sm/Fe(100) as a function of Sm coverage. The photon energy ($h\nu=135$ eV) is at the maximum of the $4d \rightarrow 4f$ resonance for the Sm divalent configuration.

face layer. The second Sm atomic layer grows on top of the first one in the divalent configuration, while the interface layer remains trivalent. After completion of the second monolayer the divalent surface layer is fully developed and any further deposition of a Sm monolayer leads to the addition of intermediate trivalent atomic layers. The asymptotic value of the curve in Fig. 4 reflects thus the surface ($2+$) to bulk ($3+$) sensitivity ratio of the measurement.

The evolution of the Sm valence with coverage here reported for Sm on Fe displays a distinct behavior from the other systems studied until now. In most other overlayer systems the reduced atomic coordination in the dilute adsorption regime is sufficient to maintain the Sm adatoms in the atomic divalent configuration. To our knowledge isolated Sm atoms have been reported to be completely trivalent only for Sm on Pd(100), reported by

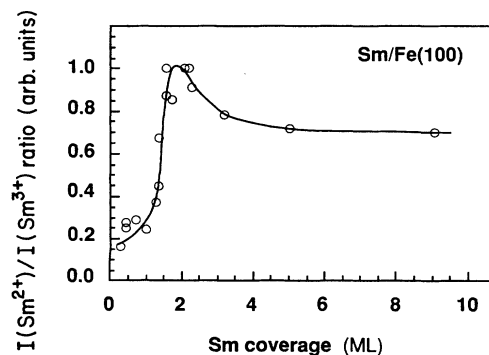


FIG. 4. Ratio of the areas of the Sm^{2+} and Sm^{3+} spectral features as a function of the Sm coverage. The ratio is arbitrary normalized to unity.

Fäldt and co-workers. In that case, however, a divalent component starts to develop just above 0.1 ML coverage. With a monolayer coverage the average Sm valence was reported to saturate to a value independent of the substrate (Si, Cu, Al, and Pd). Fäldt and co-workers attributed this behavior to the Sm-Sm interaction, leading to a degeneracy between Sm^{3+} and Sm^{2+} configuration, which prevails on the substrate interaction for a disordered monolayer. Sm on Fe(100) does not follow such a trend, remaining essentially trivalent from very low coverage up to 1 ML coverage, a result which in fact points out the importance of the interaction with the substrate. The results for Sm on Fe present some analogy with those on the ordered growth of Sm on Mo(110) studied by Stenborg and co-workers.⁸ Sm on Mo(110) is divalent at low coverage, then it undergoes several valence transitions in the submonolayer regime corresponding to different adsorption stages. An ordered Sm monolayer on Mo is completely trivalent, similarly to the case of Sm on Fe.

Some more information on the overlayer growth mode in the low coverage regime is provided by the binding energy and linewidth of the Sm^{3+} emission. The binding energy of the main Sm^{3+} peak is plotted in Fig. 5 as a function of the overlayer thickness. The Sm^{3+} features shift towards lower binding energy almost linearly with increasing coverage up to 2 ML thickness. Above 2 ML coverage the Sm^{3+} emission remains at a fixed binding energy. The value of the binding energy shift for the first two Sm monolayers on Fe compares well with other experimental observations for electropositive metals adsorbed on metals. Stenborg and Bauer¹⁴ have pointed out that the binding energy shift is mainly driven by the changes of the local adsorbate-adsorbate atomic coordination.

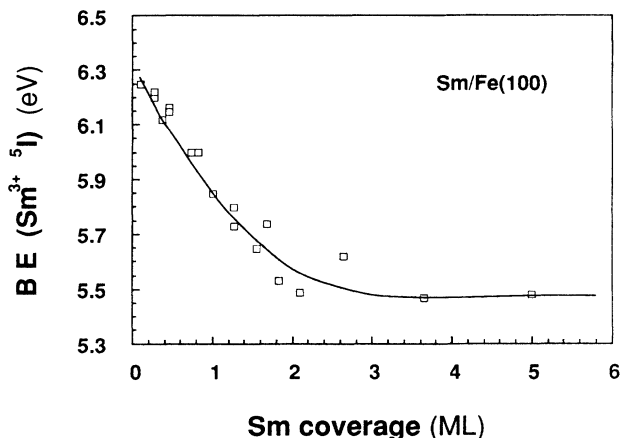


FIG. 5. Binding energy shift of the Sm^{3+} spectral peaks (main multiplet line 5I) vs Sm coverage.

The shift of the Sm^{3+} features is followed by their progressive narrowing which is completed only at 5–10 ML thickness. A similar trend, already reported for other RE overlayer systems,¹⁵ could be attributed either to strong vibrational effects or to the presence of inequivalent atomic sites at low coverage. Vibrational broadening should be significantly more pronounced for submonolayer than for bulk emission, since surface atoms should have a higher degree of vibrational freedom.¹⁶ The broadening of the Sm^{3+} $4f$ emission persists on Fe up to several monolayers of coverage indicating that vibrational excitations are probably not the only mechanism at work. We rather attribute the progressive narrowing of the Sm^{3+} emission in the 2–10-ML range to the development of short-range atomic order in the overlayer. The Sm sites at the interface are out of register with the substrate, as shown by LEED, because of the mismatch between the Sm and the Fe lattice constants. Short-range order in the Sm overlayer can presumably be gradually established away from the interface.

We briefly recall the main points discussed in this section, which are important in the following discussion of the magnetic properties. Sm grows on Fe in the layer-by-layer mode. The Sm atomic layer in contact with Fe is trivalent. Sm overlayers consisting of more than one atomic layer have trivalent configuration with a divalent topmost surface layer.

IV. MAGNETIC COUPLING

Sm is a convenient choice for studying in detail the magnetic structure of ultrathin overlayers because the Sm^{2+} surface signal is well separated from the Sm^{3+} emission of the underlying layers. The magnetic properties of the Sm/Fe system have been investigated by spin- and energy-resolved photoemission by directly sampling the polarized electronic states.

Selected spin-resolved spectra, measured at 141-eV photon energy, for various Sm coverages are reported in Fig. 6. The photoelectron spin polarization has been measured along the in-plane Fe $\langle 100 \rangle$ direction. The

low coverage spectra are dominated by the Fe $3d$ -band emission near the Fermi level. The polarized Fe $3d$ -band emission contributes mostly to the spin-up channel. With increasing coverage, the Sm^{3+} $4f$ multiplet features grow, between 5- and 10-eV binding energy, on the smooth and polarized inelastic background.

The binding energy and line shape of the Sm^{3+} emission are very similar in both spin-resolved curves. However, the Sm^{3+} intensity is not equally split between the two spin channels. The Sm^{3+} multiplet features appear mostly in the spin-down channel, demonstrating that the Sm $4f$ emission is polarized in opposite direction with respect to the Fe $3d$ bands.

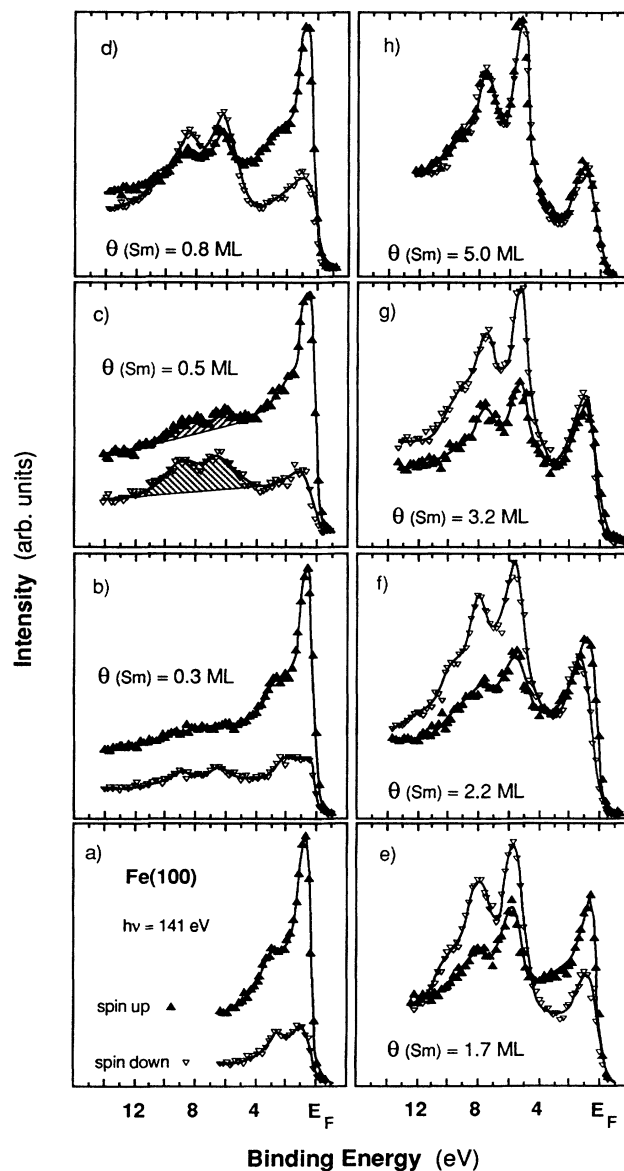


FIG. 6. Stack of spin-resolved photoemission spectra of Sm overlayers on Fe(100) as a function of the Sm thickness [$\Theta(\text{Sm})$]. In (c) the linear background used to estimate the effective polarization of the trivalent layers is also reported. All the spectra are taken at 141-eV photon energy, in normal emission, and with s -polarized light.

The Sm^{3+} effective polarization P_{eff} is $(A^\uparrow - A^\downarrow)/(A^\uparrow + A^\downarrow)$, where A^\uparrow and A^\downarrow are the areas between the two spin-resolved curves and the inelastic background (note linear background [see Fig. 6(c)]). Above 1 ML coverage the Fe valence-band contribution has to be subtracted from the spectra in order to determine the Sm^{2+} polarization. These subtractions have been performed using the spin-resolved antiresonance spectra, properly normalized to the incoming photon flux. The extracted Sm^{2+} features are found to have similar shape but different intensities in the two spin channels, showing that also the Sm surface layer has an in-plane spin component antiparallel to the Fe spin moment.

The polarization values for the $4f$ emission obtained from the photoemission spectra are plotted in Fig. 7 as a function of Sm coverage. The experimental uncertainties are larger for the Sm^{2+} polarization than for the trivalent one because the divalent signal is smaller and superimposed to the Fe $3d$ emission. For coverage up to 1 ML the Sm^{3+} photoelectron polarization is close to -50% . The Sm^{3+} signal, originating from the Sm^{3+} interface layer, remains highly polarized between 1 and 2 ML coverage. The Sm^{2+} surface layer is formed between 1 and 2 ML coverage with a polarization equal to -28% . When the third monolayer begins to be formed, the Sm^{3+} emission becomes less polarized, containing contribution both from the interface layer and from the second monolayer. At 3 ML coverage the Sm^{3+} polarization is about -28% whereas the polarization of the divalent surface layer is close to zero. At higher coverage the Sm^{2+} and Sm^{3+} emissions are not polarized. Figure 7 also contains a fitting of the experimental data assuming that the in-plane polarization of each atomic layer depends only on its distance from the interface.¹⁷ The estimated values of the polarization are all negative and equal to -47.5 , -24.7 , $-1.7 (\pm 5\%)$.

The polarization of the Sm emission proves that the Fe

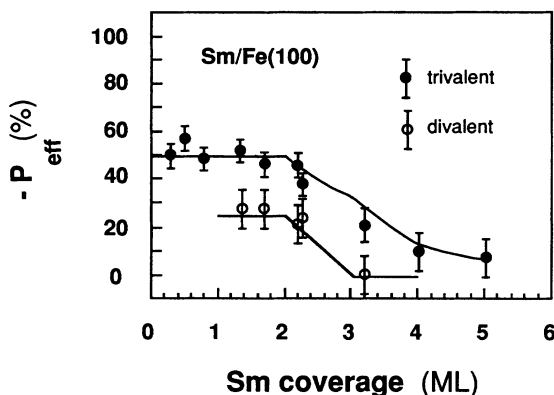


FIG. 7. Effective polarization of the divalent (open symbol) and trivalent (closed symbol) Sm layers vs Sm coverage. The dependence of the effective spin polarization of the photoemitted electrons in a model in which the in-plane magnetic order is a function only of the distance of the Sm layer from the Sm/Fe interface is also shown (solid curve).

substrate induces long-range magnetic ordering in the Sm overlayer, with a ferromagnetic component in the surface plane. The negative sign of the polarization shows that coupling between the $4f$ and the Fe $3d$ spin moment is antiparallel, as in other RE interfaces.⁶ The highly localized character of the $4f$ shell prevents its direct interaction with the Fe $3d$ states. The interaction between Sm and Fe is thought to proceed through the hybridization and spin coupling of the Fe $3d$ and Sm $5d$ states.¹⁸ In turn, the $4f$ shell acquires a spin character from the local exchange interaction with the valence electrons. Thus the $5d$ spin moment is coupled antiparallel to the Fe $3d$ moment and parallel to the $4f$ spin, producing an antiparallel spin coupling between the RE $4f$ and Fe $3d$ states. It is worthwhile to remark that the sign of the polarization is found to be negative for all the Sm monolayers. This observation shows that the in-plane spin moments of surface and bulk Sm monolayers couple themselves parallel with each other. Thus the surface magnetic structure of Sm overlayers on Fe does not present the surface-induced magnetic reconstruction reported for Gd overlayers on W(110),¹⁹ where antiparallel coupling occurs between the surface and the bulk spin moments.

The in-plane polarization of the $4f$ emission is not complete (less than 100%) at any coverage, indicating that the $4f$ spin moments are not completely aligned along the Fe $\langle 100 \rangle$ surface direction. Temperature-induced magnetic disorder as well as magnetic anisotropies which force the $4f$ spin vector out of the surface could contribute to decrease the in-plane polarization. Moreover both the Curie temperature and the magnetic anisotropies of these films may depend on their thickness.

Whatever mechanism is responsible for the incomplete polarization, *the results presented here provide clear evidence that the in-plane magnetization is not uniform within the ultrathin Sm overlayer.* The spectra of 2- and 3-ML Sm, for example, directly show that the emission from the divalent surface is much less polarized than that from the underlying trivalent layers. This observation demonstrates that *the magnetization vector near the interface changes rapidly monolayer after monolayer.* Figure 7 shows indeed that the decay of the in-plane component of the spin polarization is very fast.

The results suggest that the main parameter controlling the in-plane ferromagnetic order within the Sm overlayer reflects the interaction with Fe, being related to the distance of a given atomic layer from the interface. In fact, the spin polarization of a Sm monolayer seems to be little sensitive on the valency and on the interaction with the Sm layers deposited on top of it. Thus the polarization of the first Sm monolayer is little affected by the formation of the second Sm layer on top of it. Similarly, the polarization of the second monolayer is found to be about -28% for the Sm^{2+} (surface) and estimated about -24.7% for the Sm^{3+} (subsurface). This is remarkable since the valence electronic structure should determine the indirect $3d$ - $4f$ exchange coupling discussed before. Finally, the observation that Sm polarization becomes equal to zero, within the experimental accuracy ($\pm 5\%$), for coverage above 4 ML is obviously consistent with the fact that bulk Sm is paramagnetic at room temperature.

V. CONCLUSIONS

The growth of Sm on Fe(100) occurs in the layer-by-layer mode. The first deposited monolayer is trivalent. At higher coverage a divalent monolayer is formed on the trivalent atomic layers. The coupling to the Fe substrate induces a ferromagnetic order in the Sm atomic layers near the interface. The spin moment of the 4*f* electrons is antiparallel to the Fe 3*d* majority-spin direction. The profile of the in-plane magnetization within the Sm overlayer has been determined in the interface region.

ACKNOWLEDGMENTS

One of us (E.V.) would like to thank Professor W. Eberhardt for his interest in this work and for the kind hospitality in his group. We wish to thank S. Blügel, W. Eberhardt, and W. Gudat for stimulating discussions. The assistance of the BESSY staff is gratefully acknowledged. One of us (R.R.) was partially supported by Grant No. BMFT05 435DAB5.

¹For a review on this topic see *Handbook of the Physics and Chemistry of Rare Earths*, edited by K. A. Gschneider and L. Eyring (North-Holland, Amsterdam, 1979), Vol. 5.

²Z. S. Shan, D. J. Sellmyer, S. S. Jaswal, Y. J. Wang, and J. X. Shen, *Phys. Rev. Lett.* **63**, 449 (1989).

³Hong Fu, Masud Mansuripur, and Pierre Meystre, *Phys. Rev. Lett.* **66**, 1086 (1991).

⁴M. Taborelli, R. Allenspach, G. Boffa, and M. Landolt, *Phys. Rev. Lett.* **56**, 2869 (1986).

⁵C. Carbone and E. Kisker, *Phys. Rev. B* **36**, 1280 (1987).

⁶C. Carbone, R. Rochow, L. Braicovich, R. Jungblut, and T. Kachel, *Phys. Rev. B* **41**, 3866 (1990); C. Carbone, R. Rochow, L. Braicovich, R. Jungblut, T. Kachel, and E. Kisker, *Vacuum* **41**, 496 (1990); O. Paul, S. Toscano, W. Hürsch, and M. Landolt, *J. Magn. Magn. Mater.* **84**, L7 (1990).

⁷W. Peatman, C. Carbone, W. Gudat, W. Heinen, P. Kuske, J. Pflüger, F. Schäfers, and T. Schroeter, *Rev. Sci. Instrum.* **60**, 1445 (1989).

⁸Sm/Pd(100): Å. Fäldt, D. K. Kristensson, and H. P. Myers, *Phys. Rev. B* **37**, 2682 (1988); Sm/Cu(100): Å. Fäldt and H. P. Myers, *ibid.* **52**, 1315 (1984); J. N. Andersen, I. Chorkendorff, J. Onsgaard, J. Ghijsen, R. L. Johnson, and F. Grey, *ibid.* **37**, 4809 (1988); Sm/Mo(100): A. Stenborg, J. N. Andersen, O. Björneholm, A. Nilsson, and N. Mårtensson, *Phys. Rev. Lett.* **63**, 187 (1989); A. Stenborg, O. Björneholm, A. Nilsson, N. Mårtensson, J. N. Andersen, and C. Wigren, *Phys. Rev. B* **40**, 5916 (1989); Sm/Al(100): Å. Fäldt and H. P. Myers, *ibid.* **30**,

5481 (1984).

⁹B. Johansson, *Phys. Rev. B* **19**, 6615 (1979).

¹⁰See, for example, J. K. Lang and Y. Baer, *Solid State Commun.* **31**, 945 (1979), and references quoted therein.

¹¹J. W. Allen, L. I. Johansson, R. S. Bauer, I. Lindau, and S. B. Hagström, *Phys. Rev. Lett.* **41**, 1499 (1978); *Phys. Rev. B* **21**, 1335 (1980); W. Gudat, S. F. Alvarado, M. Campagna, and Y. Pétroff, *J. Phys. (Paris) Colloq.* **41**, C5-1 (1980).

¹²U. Fano, *Phys. Rev.* **124**, 1866 (1961).

¹³P. A. Cox, J. K. Lang, and Y. Baer, *J. Phys. F* **11**, 113 (1981); Y. Baer, J. K. Lang, and P. A. Cox, *ibid.* **F 11**, 121 (1981).

¹⁴A. Stenborg and E. Bauer, *Surf. Sci.* **211/212**, 470 (1989).

¹⁵C. Laubschat, G. Kaindl, W.-D. Schneider, B. Reihl, and N. Mårtensson, *Phys. Rev. B* **33**, 6675 (1986).

¹⁶A. Stenborg, J. N. Andersen, O. Björneholm, A. Nilsson, and N. Mårtensson, *J. Electron Spectrosc. Relat. Phenom.* **52**, 47 (1989).

¹⁷The weight of the different layers is determined by the exponential decay suffered by the escaping electrons in crossing a layer of material. We have used an escape depth of 4 Å for the 4*f* electrons coming from both the trivalent and divalent Sm atoms as derived independently from the Auger measurements.

¹⁸B. Drittler, N. Stefanou, S. Blügel, R. Zeller, and P. H. Dederichs, *Phys. Rev. B* **40**, 8203 (1989).

¹⁹D. Weller, S. F. Alvarado, W. Gudat, K. Schröder, and M. Campagna, *Phys. Rev. Lett.* **54**, 1555 (1985).